Iterative identification of stiffness parameters in a car suspension elastokinematic model

**Julien Meissonnier*, Philippe Metz*, Jean-Christophe Fauroux*,
Grigore Gogu*, Cédric Montezin****

* Laboratoire Mécanique et Ingénierie (LaMI)
Université Blaise Pascal(UBP), Institut Français de Mécanique Avancée (IFMA)
Campus de Clermont-Ferrand / Les Cézeaux
B.P.265 – F-63175 AUBIERE cedex
** Manufacture Française des Pneumatiques Michelin
Centre de Technologies de Ladoux
63040 Clermont-Ferrand

Abstract:

In this paper a new identification method of bushing stiffness parameters in car suspension mechanism is presented. This method is based on the observation of part motions in a suspension on a Kinematic and Compliance (K&C) test bench. This observation is used to compute bushing deflections for various load cases applied on the suspension. An iterative identification method has been set up and interfaced with a commercial multibody simulation software (ADAMS) in order to find a set of stiffness parameters that achieve the correlation between model and reality. This identification method is tested on a pseudo Mc Pherson suspension and on a complex multilink rear suspension. In each case, behaviour of the identified model converges towards the reference behaviour.

Keywords: Car suspension, elastokinematic, stiffness parameter identification, elastomer bushing, multibody simulation, ADAMS.

1 INTRODUCTION

The automotive industry was an early user of multibody simulation software for vehicle behaviour analysis and suspension mechanism design. The use of these tools allows to reduce the time needed to develop new suspensions. But before using a model to improve an existing vehicle, it is important to correlate the model with a real vehicle in order to ensure that modelling assumptions and model parameters are valid. That is why model correlation is a recurrent problem.

Obtaining a full correlation between a model and a given suspension is a complex task. The complex behaviour of rubber bushing used for vibration filtering is a known cause of discrepancy between model and reality [1,2]. To build a correct elastokinematic model of a given suspension, bushing stiffness must be determined. However, direct measurement of stiffness is very difficult because it requires a full disassembly. Therefore an identification method may be used to find stiffness values and attain a reliable model.

Former identification methods addressing this problem are based on the analysis of the wheel behaviour on a Kinematic and Compliance (K&C) test bench. As typical vehicle models used in industry are over complex[3], the first necessary step is to use statistical design of experiments in order to determine which

parameters influence wheel behaviour most[4]. Then, the application of optimisation routines for these parameters can be used to fit the model behaviour to experimental results [5]. The identification is then similar to a problem of optimal design [6]. These techniques imply the realisation of a high number of simulations and advanced knowledge of numerical computation is required.

The aim of this paper is to provide a more simple identification method that is no longer based solely on the observation of the wheel. This method uses observed displacements of each solid part connected by bushing in the suspension when various load cases are applied on the wheel. Section 2 presents the method used to compute part location and orientation on an assembled suspension starting from coordinate measurements of a minimum number of reference points using a portable Coordinate Measuring Machine (CMM). Based on this data, bushing deflections are computed for each load case.

To achieve simple tool for a frequent use in an engineering department, the identification method detailed in section 3 could be implemented on any commercial multibody simulation software. Usually, this type of software cannot consider stiffness parameters as unknown terms and is opaque for the user. An original approach was developed to modify iteratively an initial estimate of stiffness parameters until the behaviour of each bushing in the model is similar to experimental results.

To validate this method, a software tool has been written and tested on two different suspension architectures: a pseudo Mc Pherson front suspension and an innovative rear axle designed by Michelin in application of the Optimized Contact Patch (OCP) concept [7,8]. In these two cases, identification has been performed using numerical simulation. Finally an experimental validation is presented on a pseudo Mc Pherson. Results of this experimentation demonstrate the capability of the identification method to achieve a realistic model without prior knowledge of bushing properties.

2 FINDING BUSHING DEFLECTIONS ON AN ASSEMBLED SUSPENSION

When a vehicle is tested on a K&C test rig, the chassis is fixed on the ground and controlled forces are applied on wheels using 6 DoF actuators. During this test it is not possible to directly measure bushing deflection because functional surfaces are hidden. It is necessary to set up an indirect measuring method.

Before the vehicle is set on the K&C bench, each part of the suspension is measured separately in R_s, a coordinate system local to the solid part, and a geometric model of the solid is built. This model fully describes positions and orientations of bushings on the part using an homogenous operator. For each bushing, a local coordinate system is defined as represented in Figure 1. The position and orientation of this coordinate system relative to R_s is defined by the homogenous operator $[\mathbf{B}_{Rs}]$[9]. If we consider a bushing that links part $s1$ to part $s2$, the position and orientation of this bushing on part 1 is defined by the operator $[\mathbf{B}_{Rs1}]$, while the operator $[\mathbf{B}_{Rs2}]$ describes its position and orientation on part 2.
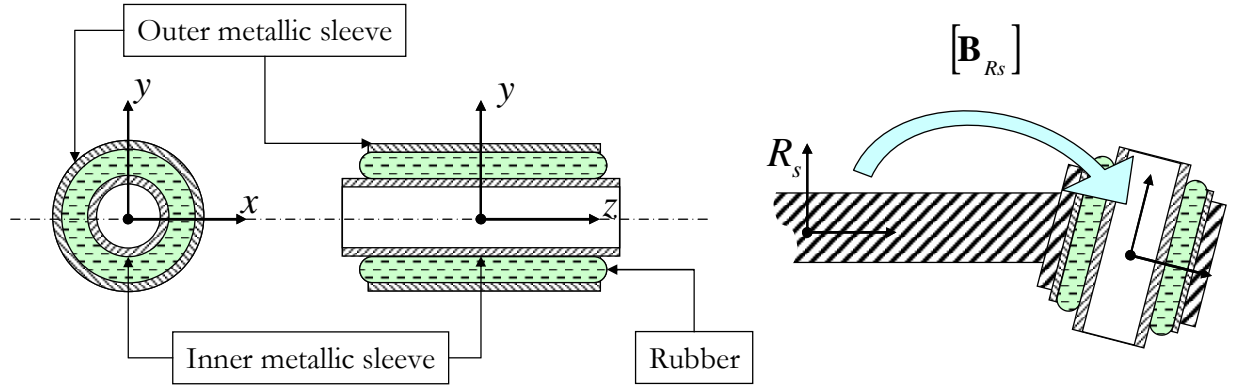
Figure 1 : Representation of coordinate system local to a bushing and location of a bushing on a part

In order to compute part location and orientation on the assembled suspension four reference points, also called "marks", are made on the part. These marks are small conic holes located on the part to ensure an easy coordinate measurement on the assembled suspension using a portable CMM, equipped with a spherical probe. The minimum number of points required to compute part location and orientation is three. However, the number of four marks has been chosen to bring reliability to the method in the event of measurement error. Before making measurements, marks should be made on the parts using a spotting drill. No precise location is required, provided the marks are sufficiently spaced from each other and accessible for coordinate measurement. Figure 2 represents, as an example, mark locations on the wishbone of a Mc Pherson suspension. After CMM measurement, each mark location is defined by a position vector:

$$\mathbf{P}_{m/Rs} = \begin{bmatrix} 1 & x_{m/Rs} & y_{m/Rs} & z_{m/Rs} \end{bmatrix}^T \qquad 1 < m < 4, \tag{1}$$

where the subscript m indicates the mark number. Once the suspension is assembled and the vehicle chassis is fixed on the bench, a load case is applied by the actuators on the wheels. Suspension reaches an equilibrium position and mark coordinates are measured in a global coordinate system R_0:

$$\mathbf{P}_{m/R0} = \begin{bmatrix} 1 & x_{m/R0} & y_{m/R0} & z_{m/R0} \end{bmatrix}^T \qquad 1 < m < 4 \tag{2}$$
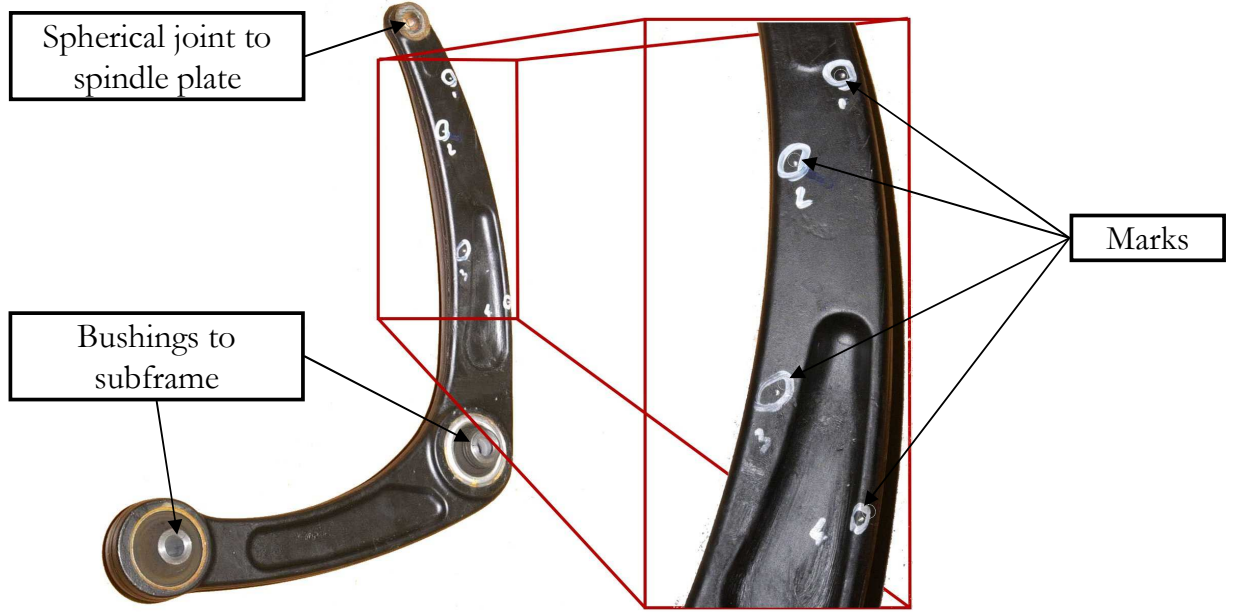
Figure 2 : Exemple of mark positioning on a suspension wishbone.

These points are used to compute the part location and orientation in the assembled suspension in the form of an operator $[A_{Rs/R0}]$. This is the absolute orientation problem [10] that consists for each part in minimizing the criterion:

$$C = \Sigma_{m=1}^{4} \left\| [\mathbf{A}_{Rs/R0}] \mathbf{P}_{m/Rs} - \mathbf{P}_{m/R0} \right\|^2 . \tag{3}$$

Based on the operator $[A_{Rs/R0}]$, it is possible to compute the elastic deflection of the bushing represented in Figure 3 with :

$$[\Delta_B] = [\mathbf{B}_{s2}]^{-1} [\mathbf{A}_{Rs2/R0}]^{-1} [\mathbf{A}_{Rs1/R0}][\mathbf{B}_{s1}]. \tag{4}$$
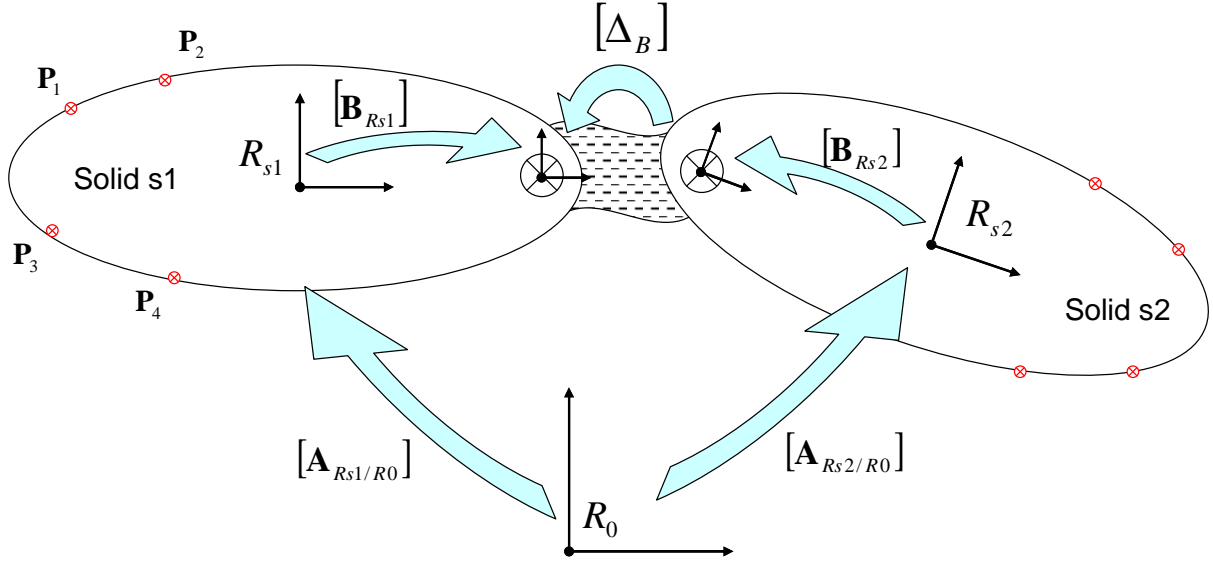
Figure 3 : Computation of bushing elastic deflection from part positions and orientations

To define a force/deflection relation for bushing B, the operator $[\Delta_B]$ has to be decomposed into 6 scalars. δ_{Tx}, δ_{Ty} and δ_{Tz} represents translational deflections, while δ_{Rx}, δ_{Ry} and δ_{Rz} represents rotational deflections with :

$$[\Delta_B] = \begin{bmatrix} 1 & 0 & 0 & 0 \\ \delta_{Tx} & a_{11} & a_{12} & a_{13} \\ \delta_{Ty} & a_{21} & a_{22} & a_{23} \\ \delta_{Tz} & a_{13} & a_{23} & a_{33} \end{bmatrix}, \tag{5}$$

and

$$\delta_{Rx} = \operatorname{atan}\left(\frac{-a_{23}}{a_{33}}\right),$$

$$\delta_{Ry} = \operatorname{atan}\left(\frac{a_{13}}{a_{33}}\right), \tag{6}$$

$$\delta_{Rz} = \operatorname{atan}\left(\frac{a_{21}}{a_{11}}\right).$$

The coordinate measurement operation is repeated for $l_{\max}$ different load cases. A load case is a set of forces applied to the wheel. It can be decomposed into three components: normal to the ground, lateral and longitudinal to the vehicle:

$$[^l\mathbf{F}_{wheel}] = [^l F_{lat} \quad {}^l F_{long} \quad {}^l F_{vert}]^T \qquad 1 < l < l_{\max}, \tag{7}$$

where the subscript l indicates the load case number. For each load case l and each bushing b, it is possible to measure mark locations and to compute the deflection values of the bushing in each direction:

$$^{l}\boldsymbol{\delta}_{b} = \begin{bmatrix} ^{l}\delta_{b,Tx} & ^{l}\delta_{b,Ty} & ^{l}\delta_{b,Tz} & ^{l}\delta_{b,Rx} & ^{l}\delta_{b,Ry} & ^{l}\delta_{b,Rz} \end{bmatrix}^{T}. \tag{8}$$

Each of these computed deflection values, $^{l}\delta_{b,Tx}$ for instance, differ from the real deflection of the bushing $^{l}\delta_{b,Tx}^{real}$ because of two distinct uncertainties. As assembly clearances are necessary to assemble the suspension, an uncertainty on geometric parameters of the elastokinematic model remains even after CMM part measurement [11]. This assembly error, named $\delta_{b,Tx}^{0}$, does not depend on the load case. The second error comes from the measurement uncertainty of the mark positions. This uncertainty leads to a random error on the computed location and orientation of parts and consequently on the bushing deflection values. This error, named $^{l}\delta_{b,Tx}^{rand}$, is different for each computed deflection. Its amplitude depends on the precision of the CMM used and the relative position of marks and bushings on parts. For any bushing deflection computed from experimental measurements, the result $^{l}\boldsymbol{\delta}_{b,Tx}$ is composed of three terms:

$$^{l}\delta_{b,Tx} \cong {}^{l}\delta_{b,Tx}^{real} + \delta_{b,Tx}^{0} + {}^{l}\delta_{b,Tx}^{rand}. \tag{9}$$

Equation (9) is not strictly verified for angular deformation as a finite angular displacement is not a vector. However this approximation is acceptable if two of the three angular deflections remain small for every load case applied to the suspension. This is generally the case for δ_{Rx} and δ_{Ry}, as a bushing is composed of two metallic cylinders (inner and outer sleeves shown in Figure 1) that bound possible angular displacements around X and Y axes.

3   STIFFNESS IDENTIFICATION METHOD

In this study, the model used to represent a bushing behaviour is a linear relation between the deflection parameters, described in equations (5) and (6), and the force and torque exerted by part 1 on 2 through bushing b. This relation is defined using six stiffness parameters:

$$\begin{aligned}
F_{b,P1\to P2} &= \begin{bmatrix} K_{b,Tx} & 0 & 0 \\ 0 & K_{b,Ty} & 0 \\ 0 & 0 & K_{b,Tz} \end{bmatrix} \begin{bmatrix} \delta_{b,Tx} \\ \delta_{b,Ty} \\ \delta_{b,Tz} \end{bmatrix} \\
M_{b,P1\to P2} &= \begin{bmatrix} K_{b,Rx} & 0 & 0 \\ 0 & K_{b,Ry} & 0 \\ 0 & 0 & K_{b,Rz} \end{bmatrix} \begin{bmatrix} \delta_{b,Rx} \\ \delta_{b,Ry} \\ \delta_{b,Rz} \end{bmatrix}
\end{aligned}. \tag{10}$$

We consider the most general case, where each stiffness parameter can be different from any other. To identify these stiffness parameters from the measured bushing deflections, it is necessary to estimate the values of forces and torques in this bushing for each load case applied on the suspension. This estimation can be done using an elastokinematic model of the mechanism. In the absence of information on the bushing stiffnesses, an initial estimation K_{0} is assigned to all stiffness parameters of the model. This model allows the computation of an equilibrium position for each load case l, and the force and torque values in each bushing b of the mechanism:

$$
^{l}\mathbf{F}_{b} = \begin{bmatrix} ^{l}F_{b,Tx} & ^{l}F_{b,Ty} & ^{l}F_{b,Tz} \end{bmatrix}^{T}
$$
$$
^{l}\mathbf{M}_{b} = \begin{bmatrix} ^{l}M_{b,Rx} & ^{l}M_{b,Ry} & ^{l}M_{b,Rz} \end{bmatrix}^{T} .
$$
(11)

The following equations are written for the computation of the translational stiffness of bushing b along the x axis, named $K_{b,Tx}$. Computations of stiffnesses in the other directions are formulated in a similar way. The aim of the identification is to find the stiffness parameter $K_{b,Tx}$ that best fits the relation:

$$
^{l}F_{b,Tx} = K_{b,Tx} \left(^{l}\delta_{b,Tx} - \delta_{b,Tx}^{0} - ^{l}\delta_{b,Tx}^{rand} \right).
$$
(12)

The force exerted on the bushing in the real suspension cannot be experimentally measured. The force computed using the elastokinematic model $^{l}F_{b,Tx}$ is considered as a good approximation of the force in the real suspension. A new value of the stiffness parameter $K_{b,Tx}$ is computed by performing a linear regression over the l_{max} ordered pairs $\left(^{l}F_{b,Tx} , ^{l}\delta_{b,Tx} \right)$, each pair corresponding to a load case. Performing the linear regression is here equivalent to minimizing the random error $^{l}\delta_{b,Tx}^{rand}$. The stiffness parameter $K_{b,Tx}$ and the assembly error δ_{0} are given by:

$$
K_{b,Tx} = \frac{\overline{\delta_{b,Tx} F_{b,Tx}} - \overline{\delta_{b,Tx}} \, \overline{F_{b,Tx}}}{\overline{\delta_{b,Tx}^{2}} - \overline{\delta_{b,Tx}}^{2}}
$$
$$
\delta_{b,Tx}^{0} = \frac{\overline{F_{b,Tx}}}{K_{b,Tx}} - \overline{\delta_{b,Tx}}
$$
, (13)

where the bar symbol stands for arithmetic mean over the load cases:

$$
\overline{a} = \frac{1}{l_{max}} \sum_{l=1}^{l_{max}} \left(^{l}a \right).
$$
(14)

This stiffness computation method is limited by the quality of measurement. If the random error on the measured deflection is greater than the real deflection, the stiffness parameter given by equation (13) is false. The statistical tool used to detect this contingency is the correlation coefficient r [12] defined by:

$$
r = \frac{\overline{\delta_{b,Tx} F_{b,Tx}} - \overline{\delta_{b,Tx}} \, \overline{F_{b,Tx}}}{\sqrt{\overline{\delta_{b,Tx}^{2}} - \overline{\delta_{b,Tx}}^{2}} \sqrt{\overline{F_{b,Tx}^{2}} - \overline{F_{b,Tx}}^{2}}} .
$$
(15)

It is proved that the value of r lies between -1 and 1. A value of r near zero indicates that the variables $^{l}\delta_{b,Tx}$ and $^{l}F_{b,Tx}$ are uncorrelated. A negative value of r occurs when the computed stiffness $K_{b,Tx}$ is negative, which is a physical nonsense in our model. It is necessary to define a value for r that defines the limit for the identifiability of the stiffness parameter. The authors chose to consider the stiffness value computed with equation (13) valid if r is superior to 0.75. If this condition is not achieved, the parameter is considered unidentifiable and the previous value is maintained.

Figure 4 represents an example of linear regression for the identification of a translational stiffness. The presented values are experimental data obtained on a pseudo Mc Pherson suspension. The amplitude of the measured deflection is 0.3 mm while the precision of the CMM used to acquire this data is around 0.1 mm. In this example, data points are a bit scattered and the correlation coefficient of 0.78 is close to the limit but the computed stiffness is near the nominal stiffness of the bushing: 13 800 N/mm.
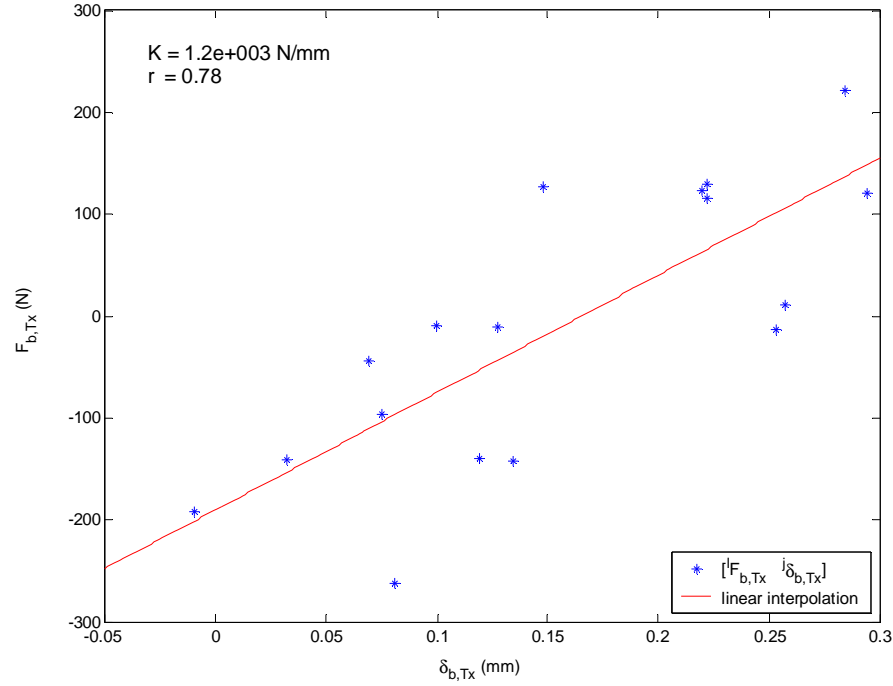

Figure 4 : Example of stiffness determination by linear regression.

In most cases, bushings present a rotational symmetry around the Z axis. Consequently, their translational and rotational stiffnesses are identical along axes x and y and the number of unknown can be reduced from six to four per bushing. To compute a single radial stiffness $K_{b,Tr}$, a weighted average is performed on $K_{b,Tx}$ and $K_{b,Ty}$ as follows:

$$w_x = \sum_{l=1}^{n} \left({}^l F_{b,Tx} - \overline{F_{b,Tx}} \right)^2 \qquad w_y = \sum_{l=1}^{n} \left({}^l F_{b,Ty} - \overline{F_{b,Ty}} \right)^2$$

$$K_{b,xTr} = \frac{1}{w_x + w_y} \left(w_x K_{b,Tx} + w_y K_{b,Ty} \right) \qquad (16)$$

where w_x and w_y are the weighting factor chosen to represent the relative importance of stiffness parameters $K_{b,Tx}$ and $K_{b,Ty}$. These terms depend on the amplitude of forces and torques applied to each direction of the bushing as the stiffness computation is more significant and precise when important forces and torques are applied, and consequently when important deflections are observed.

Initial estimation of the stiffness parameters can be very different from the real stiffnesses. As a consequence, force and torque computed in bushings may be significantly different than actual efforts in the

real suspension. An iterative process is necessary. All stiffness parameters of the elastokinematic model are modified according to the stiffnesses computed above. This new model is then used to compute new equilibrium positions for each load case and corresponding values of force and torque in the bushings.

Setting up the model equilibrium and computing stiffnesses is repeated until the convergence of the computed stiffness values is obtained. This convergence is achieved when each stiffness value computed at the iteration $i+1$ is equal to the stiffness computed at iteration i with a relative tolerance ε :

$$1-\varepsilon < \frac{K_{b,Tx,i+1}}{K_{b,Tx,i}} < 1+\varepsilon .$$
(17)

This criterion is achieved for one parameter in two cases. In first case, the parameter is not identifiable according to the correlation coefficient defined in equation (15). The second case, bushing deflections computed using model δ_{mod} at iteration i are similar to deflections in the real suspension. This affirmation is obtained from the force-deflection relation in the model and the definition of K_{i+1} :

$$
\begin{aligned}
\delta_{\text{mod}} &= \frac{F_i}{K_i} \\
F_i &= K_{i+1}\left(\delta_{\text{exp}} - \delta_0\right) \\
K_{i+1} &\cong K_i \quad \Rightarrow \quad \left(\delta_{\text{exp}} - \delta_0\right) \cong \delta_{\text{mod}}
\end{aligned}
$$
(18)

There is no formal demonstration of the convergence of the iterative process, but the convergence was observed for each identification performed during the numerical experiments. Figure 5-a represents the diagram of this identification algorithm.
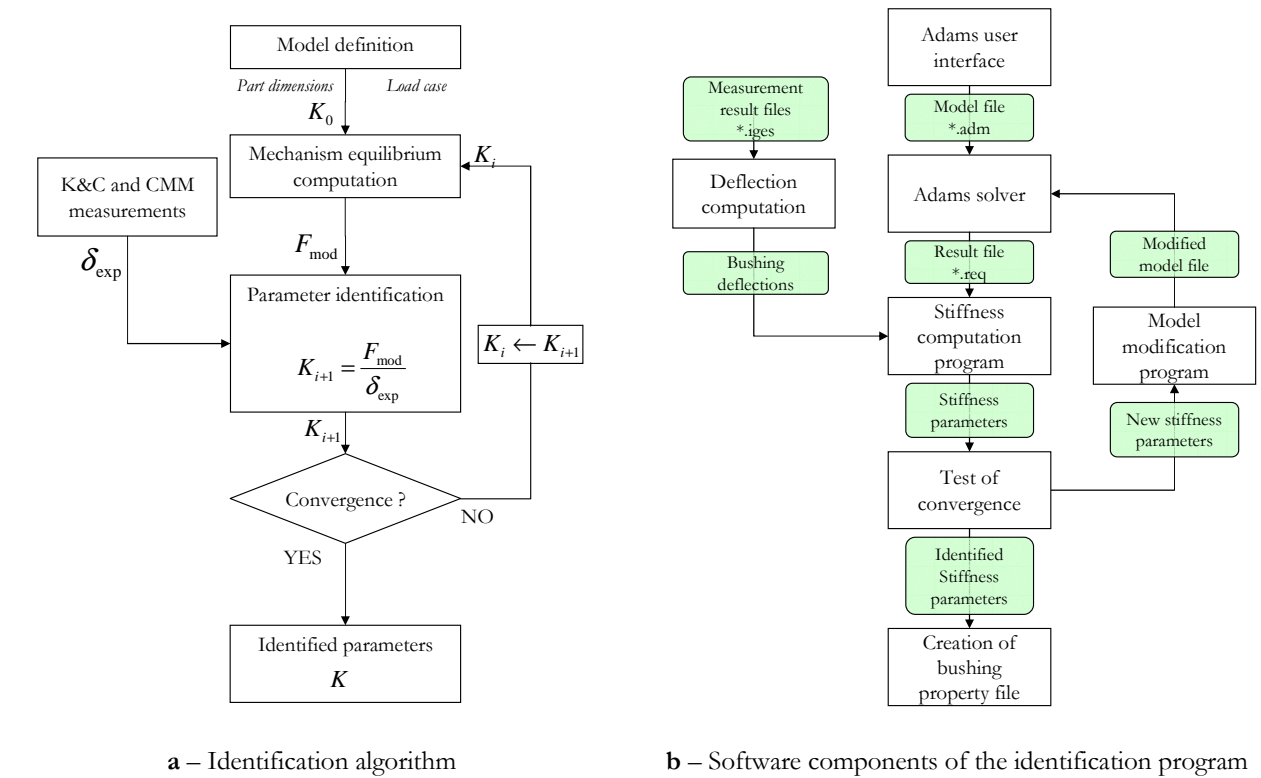
a – Identification algorithm	**b** – Software components of the identification program

Figure 5 : Implementation of the identification algorithm in a software tool.

4   NUMERICAL AND EXPERIMENTAL VALIDATION

4.1   Algorithm implementation

In order to validate the method presented, a program that performs automatically the iterative identification has been written using the Matlab programming language. The elastokinematic model is built using the commercial multibody simulation software ADAMS/Car. To compute equilibrium positions of the mechanism, this software resolves the Lagrange formulation of the equation of motion using a Newton-Raphson type algorithm [13].

At the first stage, the ADAMS user interface is used to create the initial elastokinematic model. Part dimensions are given by CMM measures and stiffness parameters are set to an arbitrary initial value. For the following examples, this initial value is 10^4 N/mm for all translational stiffnesses and 10^4 N.mm/deg for all rotational stiffnesses. The set of load cases is also described at this stage. To identify as precisely as possible stiffness parameters, these load cases should apply a load on the suspension in different directions.

When the Adams modelling phase is complete, a model file is created and sent to the ADAMS solver. This file contains all necessary information for the solver to compute an equilibrium position of the system for each load case. Once the simulation is done, the solver describes these equilibrium states in a result file. This file is automatically analysed and compared to measured bushing deflections. A new set of stiffness parameters is computed as described in the previous section.

The model file is then updated in order to use these new stiffness parameters in the bushing models. A new simulation is then ordered to the solver with a DOS command specifying the model file to use. This loop is repeated until convergence of the parameters is reached. The implementation of the identification method using the ADAMS solver is represented in Figure 5-b.

4.2 Validation on a pseudo Mc Pherson suspension using simulation data

The first application of the presented method has been made on a pseudo Mc Pherson front suspension. This axle system has the particularity of using a virtual ball joint formed by the front and rear arm instead of a wishbone. In this study, the bushings to identify are the two lower bushings linking rear and front arm to the chassis, named respectively A and B in Figure 6. With ADAMS/Car, an elastokinematic model of this suspension is built from CMM measurements made on a real suspension. A set of load cases is designed to provide a wide range of solicitations to the suspension. This load case set, described in Table 1, is a succession of vertical, lateral and longitudinal loads of various magnitudes.

In the first step, stiffness parameters are set according to the effective stiffness in the real suspension. This first model is taken as a reference and bushing deflections δ_{exp} given by the simulation are used as input data for the identification. To perform the identification, a copy of this reference model is modified to set all stiffness parameters of the bushings to the same initial estimation: 10 000 N/mm for translational stiffness and 10 000 N.mm/deg for rotational stiffness. With a tolerance ε set at 0.01, convergence is achieved in 24 iterations.
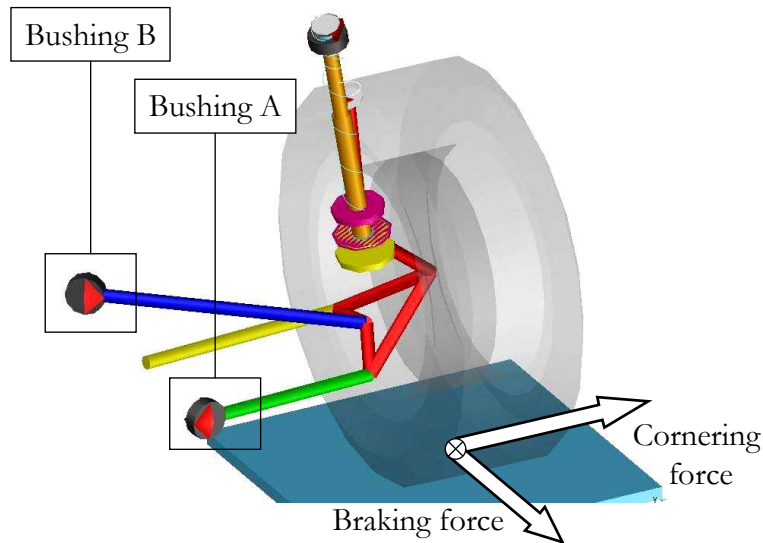

Figure 6 : elastokinematic model of the pseuso Mc Pherson suspension.

Throughout the identification process, it is verified that stiffness parameters converge to a value near the reference stiffness. However, at the end of the identification process most parameters are not exactly equal to the reference stiffness. This can be explained by the fact that several different sets of stiffness parameters can lead to a similar global behaviour. Consequently, some parameters cannot be identified independently from each other.

For instance, Figure 7 represents the evolution of computed stiffness of bushing A. In this graph, each computed stiffness is divided by the reference stiffness in order to visualise the proximity of the identified

stiffness to the ideal value with a non dimensional criterion. We can see that the translational stiffness along the X axis is correctly identified at the first iteration. This is an influent parameter for the suspension. On the other hand, the bushing is not subject to rotational deformations along the X axis. Consequently the corresponding rotational stiffness is not identifiable and the initial estimate is maintained.

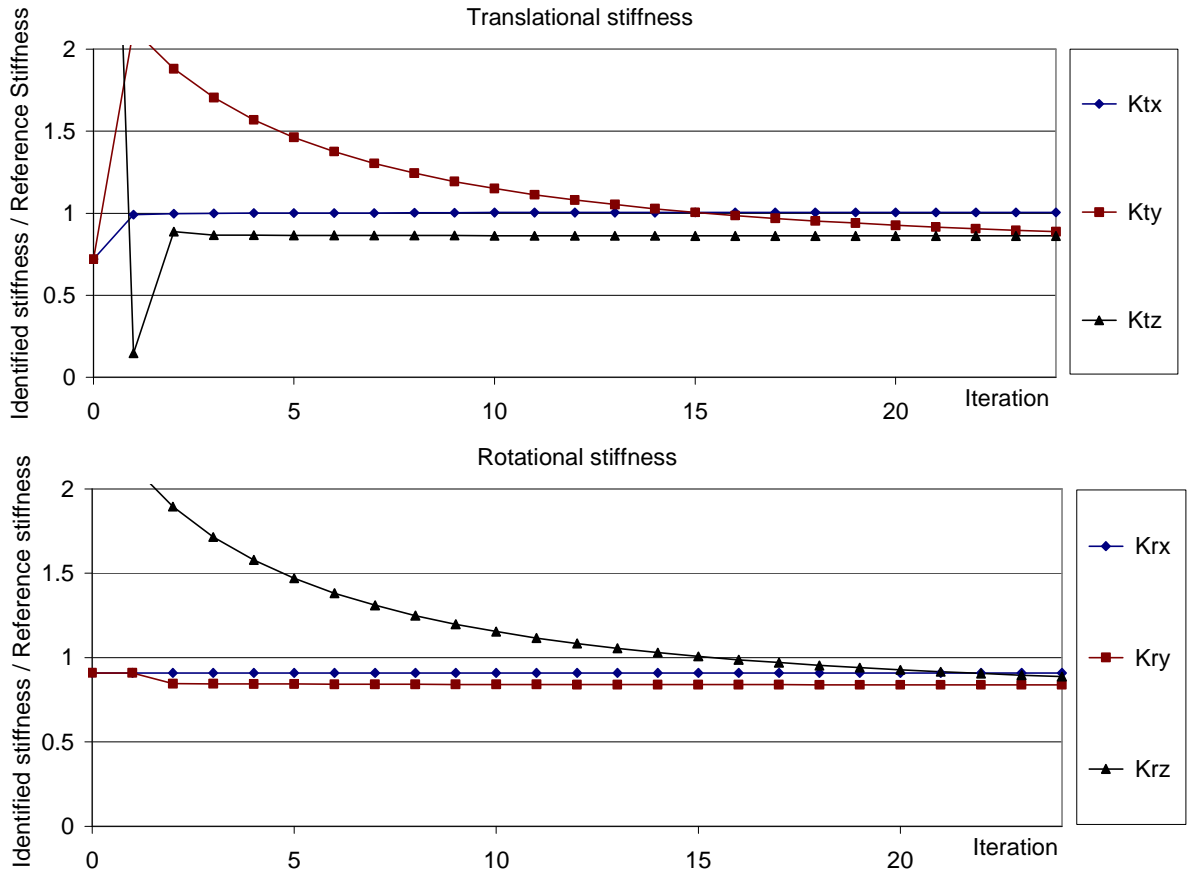|	Ktx (n/mm)	Kty (n/mm)	Ktz (n/mm)	Krx (n.mm/deg)	Kry (n.mm/deg)	Krz(n.mm/deg)
Reference stiffness	13875	13875	1370	11000	11000	4000
Inital estimation	10000	10000	10000	10000	10000	10000
Final Identified Stiffness	13959	12318	1180	10000	9223	3550
Ki/Kr	1.01	0.89	0.86	0.91	0.84	0.89

Figure 7 : Comparison of identified parameters to reference stiffness at each iteration of the identification process in bushing A

4.3   Validation using simulation data on an OCP axle

In order to test the robustness of this method to measurement uncertainties, and its reliability for complex mechanisms, the identification procedure was applied to the Optimized Contact Patch system. This patented multilink rear suspension [7,8] is characterized by an additional degree of mobility in relation to the camber

angle of the two wheels, in comparison with conventional axes. The final target consists in having negative camber when cornering, merely by the application of the ground loads on the wheel bases. This negative camber ensures the best tyre running conditions and consequently improved road holding properties. Figure 8-a presents a CAD view of this axle and Figure 8-b the corresponding elastokinematic model built with ADAMS/Car.

a- Digital mock-up of the OCP suspension
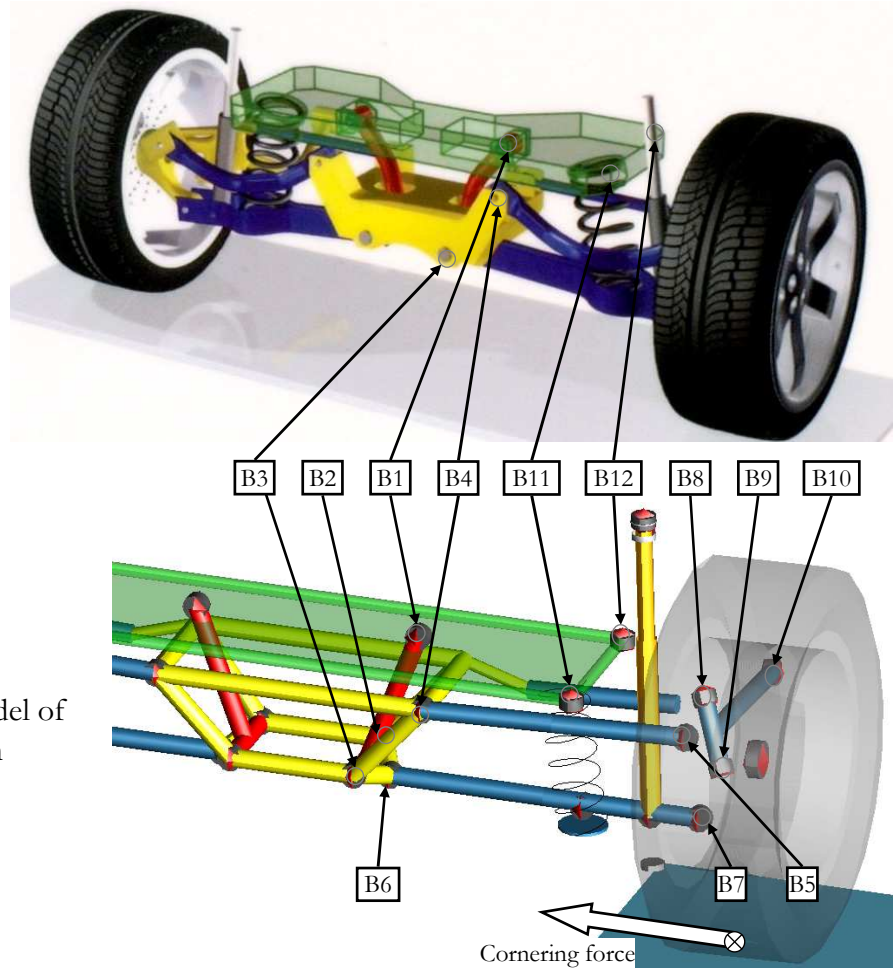
b- Elastokinematic model of the OCP suspension

Figure 8 : OCP rear axle, CAD and ADAMS/Car model.

In this identification process, the stiffnesses of twelve bushings on the left side of the axle have to be identified simultaneously under the assumption of axis symmetrical geometry, corresponding to 48 unknown parameters. A first model is used to give the reference behaviour. Four points are created on each part of the model. These points represent the marks needed to compute bushing deflections in a real suspension as described in section 2. For each load case, the coordinates of marks on the reference model are given by the simulation software.

In order to test the influence of measuring uncertainties on the identification, a random component is added to each coordinate. This noise is chosen with a normal distribution and a standard deviation of 0.05 mm. This value simulates measurement uncertainty that can be achieved with a typical portable CMM, making measurements when accessibility is difficult. These inaccurate coordinates are then used to compute part locations and bushing deflections as described in section 2.

The model to identify is geometrically identical to the reference model, but all stiffness parameters are set to 10 000 N/mm or 10 000 N mm/deg. Due to the model's complexity and the presence of noise, the convergence of the identification process is slower. In order to achieve identification in a reasonable number of iterations, the tolerance on convergence ε is set at 0.05. Convergence is then achieved after 50 iterations. During this identification, seventeen parameters are considered as non identifiable and keep their initial value.
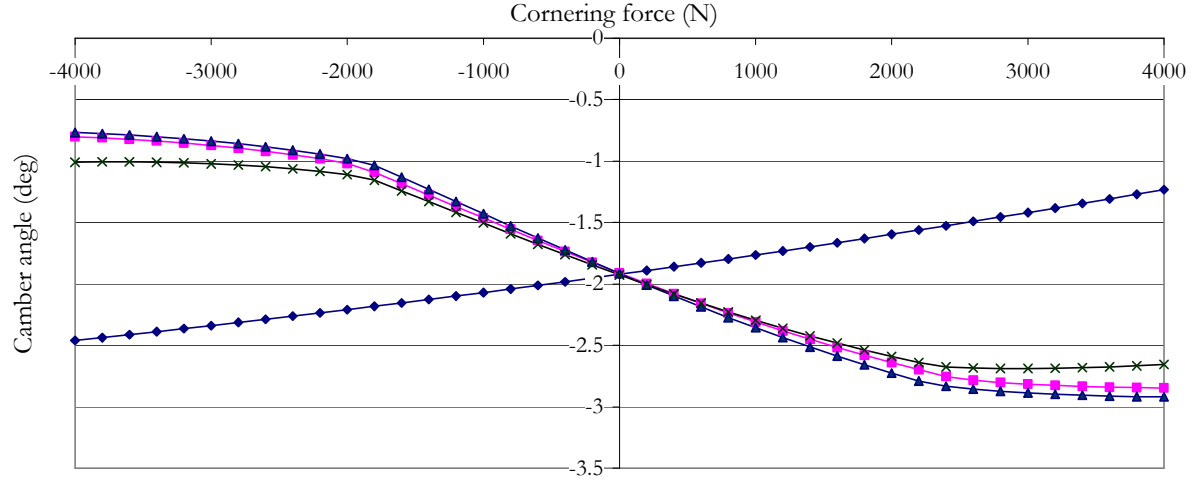
a - Camber angle under cornering force.
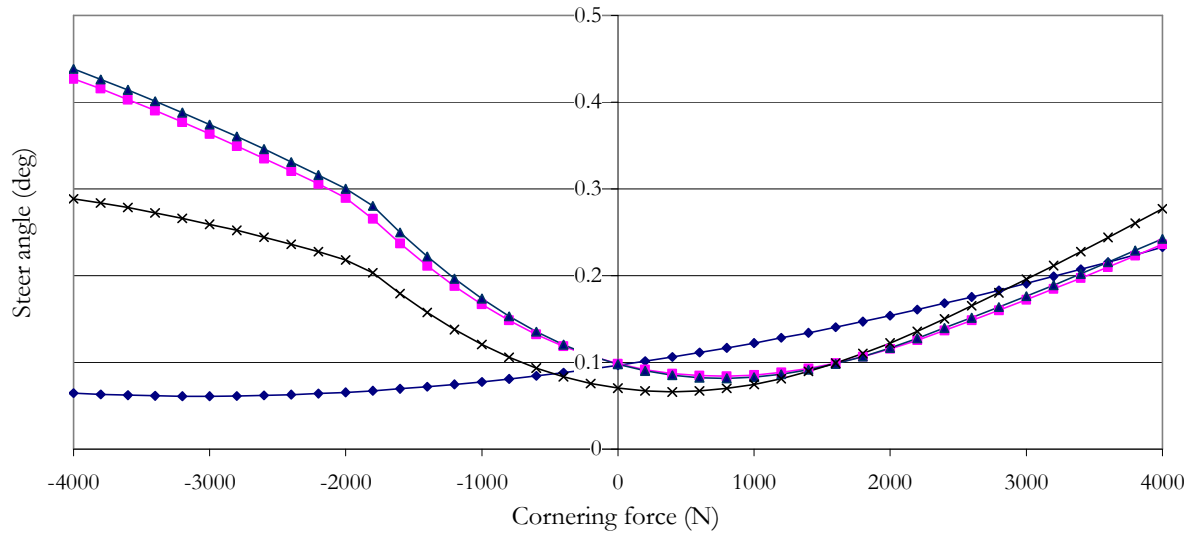
b - Steer angle under cornering force.

Model with initial stiffness   Reference model   Identification without noise   Identification with noise

Figure 9 : Wheel behaviour under cornering force for OCP models with different stiffness parameters

To estimate the quality of the identified model, wheel behaviour of the reference and identified models are compared for standard load cases such as vertical wheel travel, braking or cornering events. As an example, the graphs in Figure 9 present variations of the wheel orientation while lateral forces are applied on the wheel bases. Two supplementary models are added to the comparison. The model with the initial estimate of stiffness parameters indicates the improvement brought about by the identification. The model identified without simulated measuring noise allows us to verify the identification accuracy in the numerical experiments by considering a perfect accuracy of mark positions.

Figure 9-a represents the camber angle variation versus cornering forces applied on the wheel bases. This behaviour is especially critical for this suspension as it provides extra road holding capability to the vehicle during cornering events. The initial estimation of stiffness parameters has been made without any prior functional analysis. As a consequence, the behaviours of the reference model and the model with initial estimation of stiffness parameters are totally different. After identification in the presence of noise, variation of the camber angle is very close to the reference model. It is verified that the remaining difference is a consequence of the noise because the model identified without noise shows behaviour similar to the reference model.

Figure 9-b represents the steer angle variation versus cornering forces applied on the wheel bases. In this case, the influence of measuring uncertainties is more significant. Variation of the steer angle is reduced and may be influenced by very small bushing deflections. The improvement of measuring precision is a key factor to achieve good correlation for this particular behaviour.

4.4   Validation using experimental data on a pseudo Mc Pherson suspension

Experimental validation for the proposed method was made on a pseudo Mc Pherson suspension. This suspension is identical to the one presented in section 4.2. Figure 10 reproduces a photo of the experimental setting. Parts of the suspension (**c**) are attached to a mechanically welded frame that reproduces the original vehicle attachment points (**b**). This frame is fixed on the K&C test rig and the spindle is linked to the bench actuators (**e**). While applying controlled forces and torques, the K&C test rig measures the wheel motion with a computer vision system (**d**). The set of load cases applied on the spindle for the identification is described in Table 2. The portable CMM (**a**) is fixed on the test rig in front of the suspension to allow mark coordinate measurement.
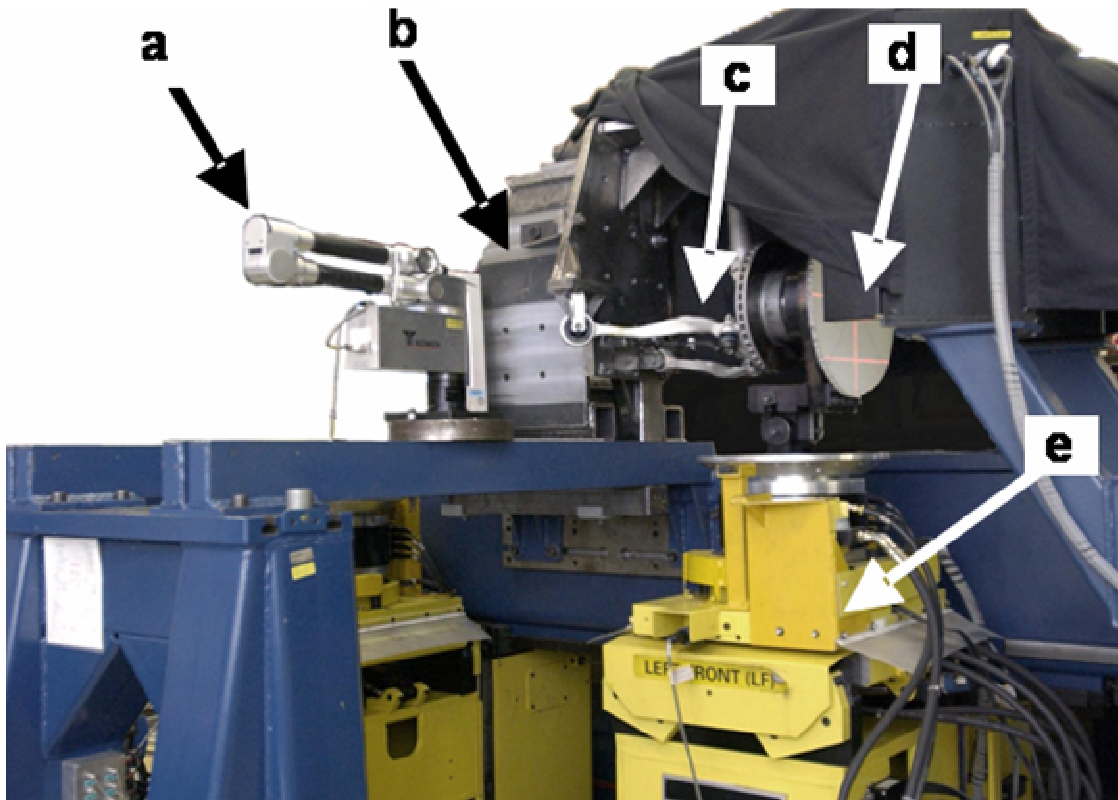
Figure 10 : Experimental setting of a pseudo Mc Pherson suspension on a K&C testbench.

Before assembling the mechanism, bushings of the front and rear arms (bushings A and B as defined in Figure 6) have been measured separately. They are used to build the most representative elastokinematic model possible prior to identification. Despite this fact, some differences remain between the behaviour of the model and the behaviour measured on the K&C test rig.

Identification is performed using 10 000 N/mm and 10 000 N mm/deg as initial stiffness estimation on both bushings. Identified stiffnesses are compared to nominal stiffnesses in Table 3. The main difference between these parameter sets lies in the translational stiffness of bushing A. The nominal value of K_{tx} is 13 000 N/mm while the identified value is 7 300 N/mm. Two reasons can be given for this major difference. First, the effective stiffness may be different from the nominal value because of manufacturing dispersion, environmental parameters (temperature …), rubber aging and rubber behaviour under multi axial load. Secondly, the identified parameter represents a global stiffness that takes into account deflections of the bushing and of surrounding parts subject to elastic deflections (bolted assembly, chassis, suspension arm).

This modification explains the improvement of the behaviour that can be seen in Figure 11-a. This graph presents the steer angle versus cornering force applied on the wheel,and a precise correlation is observed for the identified model. The hysteresis that can be seen in this graph indicates the presence of dry friction and a plastic behaviour of rubber elements. These phenomena are not represented in our model and should be taken into account for a better accuracy.

The graph in Figure 11-b presents the steer angle versus braking force. The identified model is closer to the real behaviour than the original model. However, correlation is not perfect. This particular behaviour

shows the limits of the model based on the assumption of non deformable parts. It is verified that representing the elastic deformation of the tie rod improves the correlation.

The wheel behaviour during vertical motion has also been tested. For this loading, a good correlation was noticed between the real axle and the unidentified model, and the stiffness identification did not bring significant changes. In that case, wheel behaviour depends mainly on the geometry of the parts and on the suspension spring.

This experimental validation demonstrates that the proposed identification method allows the definition of a representative elastokinematic model of a suspension without prior information on bushings.
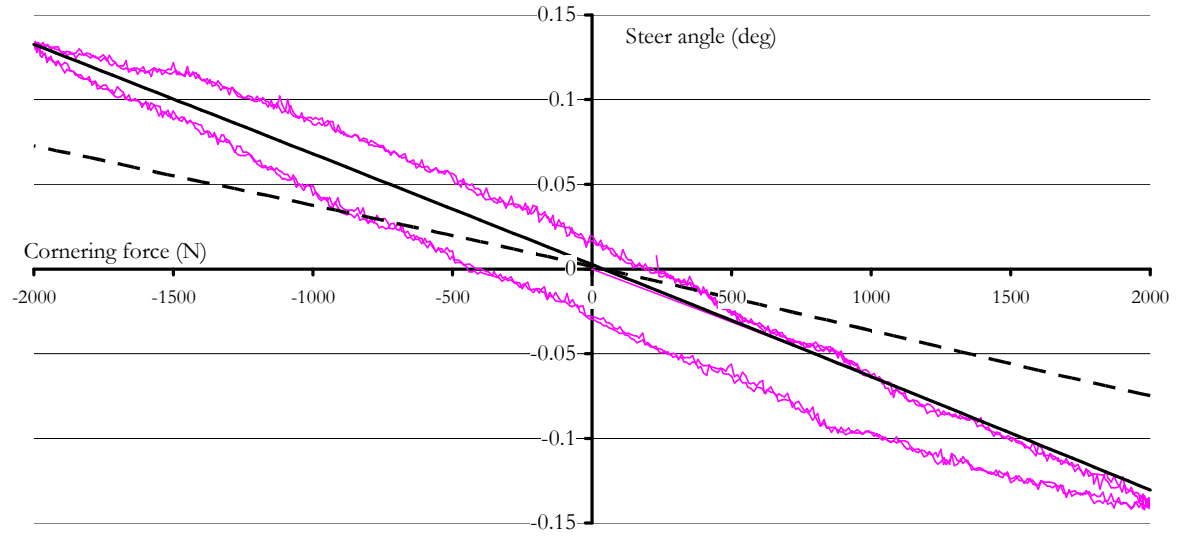
a - Steer angle under cornering force.
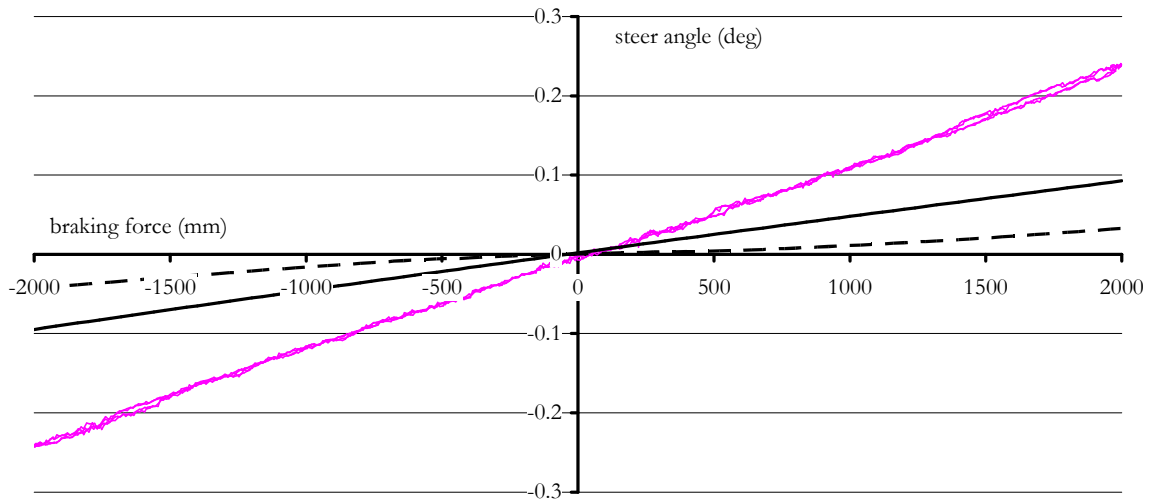
b - Steer angle under braking force.

―――― Experimental data ― ― Model with nominal stiffnesses ―――― Model with identified stiffnesses

Figure 11 : Comparison of experimental data and elastokinematic models.

5   CONCLUSION

In this article a new method for stiffness parameter identification in vehicle suspension mechanisms is proposed. This method is based on the observation of each part displacement during a Kinematic and Compliance test. The only required additional device is a portable CMM. The algorithm used is voluntarily simple and can be applied to any type of suspension.

This identification method has been tested using numerical simulation on two different suspension architectures. These experiments showed that this method was capable of identifying a large number of parameters simultaneously even in the presence of measuring uncertainties. Experimental validation demonstrated that identification brings a significant improvement of the correlation between a real suspension and its elastokinematic model.

The main limitation of this method remains in its capability to measure precisely coordinates of reference points in the mechanism. When a bushing deflection is smaller than the measuring precision, the corresponding stiffness may not be identifiable.

The other limitation comes from the use of multibody simulation software to compute forces exerted on the bushings. As a consequence, a time consuming iterative process is necessary to compute the stiffness parameters. Based on the hypothesis of linear force-deflection relation, the direct solution of this identification problem is possible in a non iterative form. This solution will be the focus of a future work.

ACKNOWLEDGMENT

REFERENCES

1   M.V. Blundell. Influence of rubber bush compliance on vehicle suspension movement. Journal of Material & Design, 19 (1997), p 29-37

2   D. Tener, C. Eichler, M. White. Bushing Modeling in ADAMS using Test and ABAQUS models. Mechanical Dynamics 2002 User Conference, May 2002.

3   R.S. Sharp. Computer code for road vehicle dynamic models.Proc of Autotech '91, Birmingham, November 1991, paper 427/16/064.

4   P.S Rao, D. Roccaforte, R. Campbell. Developing an ADAMS model of an Automobile using test data. SAE Technical paper # 2002-01-1567

5   E. Rocca ,R. Russo. A feasibility study on elastokinematic parameter identification for a multilink suspension. Journal of Automobile Engineering, February 2002, Vol. 216, p. 153-160.

6   R. Sancibrian, P.Garcia, F. Viadero, A. Fernandez. Suspension system vehicle design using a local optimization procedure. Proc. of ASME International Design Egineering Technical Conference, technical paper # DETC2005-84441. September 2005, Long Beach, California, USA.

7   L. Heuze, P. Ray, G. Gogu, L. Serra, F. Andre. Design studies for a new suspension mechanism. Journal of Automobile Engineering. 2003, Vol 217 N°7, p.529-535.

8   F. Andre, M.Blondelet, G.Gogu, L.Serra. Vehicle wheel suspension device. Patent WO2004009383. Michelin recherche et technique S.A, January 29 2004.

9   G. Gogu, P. Coiffet. Représentation du mouvement des corps solides. Editions Hermes, Paris, France, 1996, p.63-80. ISBN : 2-86601-531-2.

10   D.W. Eggert, A. Lorusso, R.B. Fisher. Estimating 3-D rigid body transformations: a comparisonof four major algorithms. Machine Vision and Applications, 1997, Volume 9, Numbers 5-6, p 272–290

11   J. Meissonnier, J.C. Fauroux, C. Montezin, G. Gogu. Identification des paramètres géométriques du mécanisme de liaison au sol d'un véhicule automobile. Proc. of 17e Congrès Français de mécanique, paper #311. August, 2005 Troyes, France.

12   W.H.Press, S.A.Teukolsky, W.T.Vetterling, B.P.Flannery. Numerical Recipies in Fortran 77. Cambridge university press, 1992, p630-633. ISBN : 0 521 43064.

13   J.B. McConville, J.F. McGrath. Introduction to ADAMS Theory. Mechanical Dynamics, Inc., paper #31-KB8788. May 2, 1997.

Table 1 : Set of load cases used to numerically test the identification method

Load case #	Vertical force (N)	Lateral force (N)	Longitudinal force (N)
1	1500	0	0
2	3000	0	0
3	4500	0	0
4	6000	0	0
5	7500	0	0
6	4500	-4000	0
7	4500	-2000	0
8	4500	2000	0
9	4500	4000	0
10	4500	0	-4000
11	4500	0	-2000
12	4500	0	2000
13	4500	0	4000

Table 2 : Set of load cases using for the experimental validation of the identification method

Load case #	Vertical force (N)	Lateral force (N)	Longitudinal force (N)
1	4500	0	0
2	5980	0	0
3	7500	0	0
4	3030	0	0
5	1510	0	0
6	4600	1000	0
7	4340	-1000	0
8	4480	0	1000
9	4470	0	-1000
10	5873	1000	0
11	5950	-1000	0
12	5920	0	1000
13	5920	0	-1000
14	3370	1000	0
15	2780	-1000	0

16	3040	0	1000
17	3090	0	-1000

Table 3: Nominal and identified bushing stiffnesses of the pseudo Mc Pherson suspension.

Bushing A	Ktx (n/mm)	Kty (n/mm)	Ktz (n/mm)	Krx (n.mm/deg)	Kry (n.mm/deg)	Krz (n.mm/deg)
Nominal stiffness	1300	13000	1370	11000	11000	4000
Identified Stiffness	7298	10000	10000	10000	6831	5066

Bushing B	Ktx (n/mm)	Kty (n/mm)	Ktz (n/mm)	Krx (n.mm/deg)	Kry (n.mm/deg)	Krz (n.mm/deg)
Nominal stiffness	310	2400	180	4500	1100	1600
Identified Stiffness	365	500	10000	10000	3404	4823